Probing light sterile neutrino signatures at reactor and Spallation Neutron Source neutrino experiments

T.S. Kosmas [1],* D.K. Papoulias [1],† M. Tórtola [2],‡ and J.W.F. Valle [2]§

[1] *Theoretical Physics Section, University of Ioannina, GR-45110 Ioannina, Greece and*
[2] *AHEP Group, Instituto de Física Corpuscular – C.S.I.C./Universitat de València*
Edificio de Institutos de Paterna, C/Catedratico José Beltrán, 2 E-46980 Paterna (València) - Spain

We investigate the impact of a fourth sterile neutrino at reactor and Spallation Neutron Source neutrino detectors. Specifically, we explore the discovery potential of the TEXONO and COHERENT experiments to subleading sterile neutrino effects through the measurement of the coherent elastic neutrino-nucleus scattering event rate. Our dedicated χ^2-sensitivity analysis employs realistic nuclear structure calculations adequate for high purity sub-keV threshold Germanium detectors.

I. INTRODUCTION

Recently, several neutrino experiments have been designed to operate with exceptional high sensitivities in order to detect neutral-current coherent elastic neutrino-nucleus scattering (CEνNS) events [1, 2] for the first time [3, 4]. Potential deviations from the standard model (SM) expectations would provide a glimpse on new physics [5–7]. Indeed, the existence of a fourth sterile neutrino could be probed in ultralow threshold neutrino-nucleus coherent scattering, since it would generate tiny modifications in the final neutrino spectrum [8, 9]. The purely neutral character of CEνNS provides an important advantage [10–12], compared to neutrino-electron scattering since there is no need for disentangling the sterile neutrino mixing from that of the active neutrinos [13].

On the other hand the solid evidence for neutrino oscillations implied by current solar and atmospheric data, and confirmed by reactor and accelerator neutrino experiments [14–17] still leaves some loopholes. These come in the form of controversial anomalies which do not fit in the three-neutrino oscillation paradigm. The Gallium [18, 19], LSND [20, 21], and MiniBooNE [22–24] anomalies, as well as the new predictions for reactor neutrino fluxes [25–27] have raised speculations on whether the actual number of neutrinos could exceed three. Taken at face value, these have suggested the possible existence of at least one sterile neutrino with new mixings to the three active neutrinos. The indicated squared mass splittings are of the order of $1\,\mathrm{eV}^2$ [28, 29]. Following earlier theoretical [30, 31] and phenomenological considerations [32], the possible existence of a fourth neutrino has drawn a lot of attention and many recent studies have been carried out [33–37]. In fact, an arbitrary number of $\mathrm{SU(2)_L}$ singlet fermions are present in the generalized type I seesaw mechanism [38] such as realized in low-scale seesaw schemes [39–42]. If it exists, the sterile neutrino is expected to take part in neutrino oscillations. Notice however that, despite the limits on the number of sterile neutrino states coming from cosmology [43], depending on the active-sterile mixing strength and their corresponding mass scale, such cosmological constraints may be adequately fulfilled [44]. Furthermore, sterile neutrino states may induce a number of processes with important phenomenological consequences to solar [45], reactor [46–48] and accelerator [49] neutrino oscillations at the sub-eV scale, possible neutrino electromagnetic interactions at the eV scale [50], dark matter at the keV scale [51, 52], etc. Moreover, the impact of a light sterile neutrino on the neutrinoless double beta-decay and single beta-decay processes has also received some attention [53–55].

Here we examine the possibility of probing light sterile neutrinos at short-baseline CEνNS experiments operating with nuclear detectors of low-threshold capabilities [56–58]. A number of experiments are now planned in order to probe possible oscillation features due to the presence of sterile neutrinos. Specifically we examine the observation potential of the COHERENT experiment at Oak Ridge [59] and the TEXONO experiment in Taiwan [60, 61]. Other relevant projects looking for this signature are the νGeN [62] and the GEMMA [63] experiments in Russia, as well as the CONNIE project in Brazil [64, 65] and the MINER experiment at Texas A&M University [66]. Notable efforts aiming at observing CEνNS by using cryogenic detector techniques include the Ricochet [67] and the ν-cleus [68] experiments. Our calculations are performed using advanced nuclear physics techniques, such as the quasiparticle random phase approximation (QRPA), in which the required nuclear form factors are obtained with high accuracy [69]. We also address the quenching effects which are crucial in order to provide realistic results [70]. For the specific case of the aforementioned reactor and spallation neutron source (SNS) experiments, we perform a χ^2 sensitivity analysis to explore the possibility that the detection of CEνNS [71–73] constitutes an efficient probe for sterile neutrino searches at low energies.

The paper has been organized as follows. We first go through a brief description of the relevant formalism of CEνNS including sterile neutrinos in Sec. II. In Sec. III we summarise the main features of the relevant experiments, such as TEXONO and COHERENT, necessary

* hkosmas@uoi.gr
† dimpap@cc.uoi.gr
‡ mariam@ific.uv.es
§ valle@ific.uv.es, http://astroparticles.es/

for our work. In Sec. IV we discuss the impact of a light sterile neutrino in neutrino-nucleus scattering. The results of our calculations are discussed in Sec. V, where we extract the expected sensitivities on the model parameters. Finally, in Sec. VI we close with a summary of our main conclusions.

II. COHERENT ELASTIC NEUTRINO-NUCLEUS SCATTERING

At low and intermediate energies, considered in the present study, the neutral-current neutrino-nucleus processes are described by the matrix elements of an effective interaction Hamiltonian, written in terms of the leptonic $\hat{j}^{lept}_\mu$ and hadronic (nuclear) $\hat{\mathcal{J}}^\mu$ currents as

$$\langle f|\hat{H}_{eff}|i\rangle = \frac{G_F}{\sqrt{2}} \int d^3\mathbf{x}\, \langle \ell_f|\hat{j}^{lept}_\mu|\ell_i\rangle \langle J_f|\hat{\mathcal{J}}^\mu(\mathbf{x})|J_i\rangle\,, \quad (1)$$

where G_F is the Fermi constant. The matrix element of the leptonic current, between an initial $|\ell_i\rangle$ and a final lepton state $|\ell_f\rangle$ takes the usual V-A form

$$\langle \ell_f|\hat{j}^{lept}_\mu|\ell_i\rangle = \bar{\nu}_\alpha \gamma_\mu (1-\gamma_5)\nu_\alpha\, e^{-i\mathbf{q}\cdot\mathbf{x}}\,, \quad (2)$$

with $\alpha = \{e, \mu, \tau\}$ being the neutrino flavor and $\mathbf{q}$ denoting the three momentum transfer. The hadronic matrix element is obtained through a multipole decomposition as described in Refs. [74, 75]. Then, the differential cross section with respect to the scattering angle θ, for the CEνNS ($gs \to gs$ transitions) off a spherical spin-zero nucleus, reads [5, 69]

$$\left(\frac{d\sigma}{d\cos\theta}\right)_{\text{SM}} = \frac{G_F^2}{2\pi} E_\nu^2 \,(1+\cos\theta) \left|\langle gs||\hat{\mathcal{M}}_{00}(Q)||gs\rangle\right|^2 . \quad (3)$$

The coherent nuclear matrix element is written in terms of the left- and right-handed couplings of the u- and d-quarks to the Z-boson as [5]

$$\begin{aligned}\left|\langle gs||\hat{\mathcal{M}}_{00}(Q)||gs\rangle\right| &= \int d^3r\, j_0(|\mathbf{q}|r) \\ \times\Big\{ &\left[2(g^{u,L}_{\alpha\alpha} + g^{u,R}_{\alpha\alpha}) + (g^{d,L}_{\alpha\alpha} + g^{d,R}_{\alpha\alpha})\right] \rho_p(r) \\ &+ \left[(g^{u,L}_{\alpha\alpha} + g^{u,R}_{\alpha\alpha}) + 2(g^{d,L}_{\alpha\alpha} + g^{d,R}_{\alpha\alpha})\right] \rho_n(r) \Big\}\,,\end{aligned} \quad (4)$$

where the notation $r = |\mathbf{x}|$ has been introduced. In the latter expression, $\rho_p(r)$ and $\rho_n(r)$ are the corresponding proton and neutron charge density distributions computed through realistic nuclear structure calculations in the context of the QRPA method. In such calculations, the finite nucleon and nuclear size are taken into consideration by weighting the differential cross section with corrections provided by the associated proton (neutron) nuclear form factors $F_{Z(N)}(Q^2)$ that depend on the square of the four momentum transfer

$$-q_\mu q^\mu = Q^2 = 2E_\nu^2 (1-\cos\theta)\,, \quad (5)$$

or $Q = 2E_\nu \sin(\theta/2)$. In Eq.(4), the u- and d-quark couplings to the Z-boson include the relevant radiative corrections, through the expressions

$$\begin{aligned} g^{u,L}_{\alpha\alpha} &= \rho^{NC}_{\nu N}\left(\frac{1}{2} - \frac{2}{3}\hat{\kappa}_{\nu N}\hat{s}^2_Z\right) + \lambda^{u,L}\,, \\ g^{d,L}_{\alpha\alpha} &= \rho^{NC}_{\nu N}\left(-\frac{1}{2} + \frac{1}{3}\hat{\kappa}_{\nu N}\hat{s}^2_Z\right) + \lambda^{d,L}\,, \\ g^{u,R}_{\alpha\alpha} &= \rho^{NC}_{\nu N}\left(-\frac{2}{3}\hat{\kappa}_{\nu N}\hat{s}^2_Z\right) + \lambda^{u,R}\,, \\ g^{d,R}_{\alpha\alpha} &= \rho^{NC}_{\nu N}\left(\frac{1}{3}\hat{\kappa}_{\nu N}\hat{s}^2_Z\right) + \lambda^{d,R}\,, \end{aligned} \quad (6)$$

with $\hat{s}^2_Z = \sin^2\theta_W = 0.23120$, $\rho^{NC}_{\nu N} = 1.0086$, $\hat{\kappa}_{\nu N} = 0.9978$, $\lambda^{u,L} = -0.0031$, $\lambda^{d,L} = -0.0025$ and $\lambda^{d,R} = 2\lambda^{u,R} = 7.5 \times 10^{-5}$ [76].

A. Nuclear physics calculations

It can be noticed that the CEνNS cross section is rather sensitive to the neutron form factor, calculable in the context of a nuclear structure model. In this work, the reliability of the evaluated cross sections is maximized by performing QRPA calculations, incorporating realistic strong nuclear forces within the framework of a comprehensive phenomenological meson-exchange theory for the reliable description of the nucleon-nucleon interaction. Our QRPA code, for the two-nucleon residual interaction utilizes the C-D version of the well-known Bonn potential [77, 78]. This way, the invariance under any rotation in isospin space, is reproduced accurately. The off shell behaviour of Bonn C-D is based upon the relativistic Feynman amplitudes for meson-exchange ($\eta, \pi, \rho, \omega, \sigma$ and ϕ mesons in our case), a fact that has attractive consequences in nuclear structure applications [79].

Motivated by its successful application on similar calculations for various semileptonic nuclear processes [80–83], the QRPA method is employed in this work to construct explicitly the nuclear ground state, $|gs\rangle \equiv |0^+\rangle$, of the studied even-even isotope (^{76}Ge in our case) through the numerical solution of the BCS equations. The vector proton (neutron) nuclear form factors are evaluated as

$$F_{N_n}(Q^2) = \frac{1}{N_n}\sum_j \sqrt{2j+1}\,\langle j|j_0(|\mathbf{q}|r)|j\rangle \left(\upsilon^j_{N_n}\right)^2\,, \quad (7)$$

where $N_n = Z$ (or N) and $\upsilon^j_{N_n}$ denotes the occupation probability amplitude of the jth single-nucleon orbit (see e.g. Ref. [69]).

III. EXPERIMENTAL SETUPS

A. Reactor neutrino experiments

Recently, it became feasible to detect neutrino-nucleus scattering events by using high purity germanium-based detectors (HPGe detector) [56, 70]. In this work, we are interested in the possibility of probing the existence of a fourth light sterile neutrino through potential deviations on the low-energy CEνNS measurements at reactor neutrino experimental facilities, such as TEXONO [60, 61], νGeN [62], GEMMA [63], CONNIE [64, 65] and MINER [66]. We have considered as reference experimental setup 1 kg of ^{76}Ge detector and a detection threshold of 100 eV$_{\text{ee}}$ [1]. We note, however, that the absence of precise information regarding the fuel composition restricts us to take into account only the dominant component of the antineutrino spectrum provided by ^{235}U. In this respect, for the present study we assume a typical flux of $\Phi_{\bar{\nu}_e} \sim 10^{13}\, \nu\, \text{s}^{-1}\, \text{cm}^{-2}$ for a detector located at 28 m from the 2.9 GW reactor core. In order to estimate the emitted $\bar{\nu}_e$ energy-distribution, $\eta^{\text{react}}_{\bar{\nu}_e}(E_\nu)$, for energies above 2 MeV, existing experimental data from Ref. [26] are employed, while for energies $E_{\bar{\nu}_e} < 2$ MeV existing theoretical estimations [84] are assumed.

B. Spallation Neutron Source experiments

The Spallation Neutron Source at Oak Ridge [1] has been recently considered as a promising facility to measure CEνNS events within the SM [4, 69] as well as to explore exotic neutrino properties [5–7]. The COHERENT experiment [59] aims to use intense neutrino beams (of the order of $\Phi_{\nu_\alpha} \sim 10^7\, \nu\, \text{s}^{-1}\text{cm}^{-2}$ per flavor) resulting from pion decay. Specifically, the stopped-pion neutrino beam consists of: (i) monochromatic muon-neutrino ν_μ flux with energy 29.9 MeV produced via pion decay at rest $\pi^+ \to \mu^+ \nu_\mu$ within $\tau = 26\,\text{ns}$ (prompt flux) and (ii) electron neutrinos, ν_e, and muon antineutrinos, $\bar{\nu}_\mu$, that are emitted from the muon-decay $\mu^+ \to \nu_e e^+ \bar{\nu}_\mu$ within $\tau = 2.2\,\mu\text{s}$ (delayed flux) [85]. The delayed flux is described by the well-known normalized distributions [86, 87]

$$\begin{aligned}
\eta^{\text{SNS}}_{\nu_e}(E_\nu) =& 96 E_\nu^2 M_\mu^{-4} \left(M_\mu - 2E_\nu\right) , \\
\eta^{\text{SNS}}_{\bar{\nu}_\mu}(E_\nu) =& 16 E_\nu^2 M_\mu^{-4} \left(3M_\mu - 4E_\nu\right) ,
\end{aligned} \tag{8}$$

with $E_\nu^{\max} = M_\mu/2$ and $M_\mu = 105.6\,\text{MeV}$ denoting the muon rest mass.

In this work, the calculation is performed for two cases corresponding to (i) the "current" configuration: a (^{20}Ne, ^{40}Ar, ^{76}Ge, ^{132}Xe) target with mass (391, 456, 100, 100) kg located at (46, 46, 20, 40) m from the source with energy threshold of (30, 20, 10, 8) keV$_{\text{nr}}$ and a running time of 2.4×10^7s, and (ii) the "future" configuration: 1 ton of detector mass located at 20 m from the source with energy threshold 1 keV$_{\text{nr}}$ and 1 year of data taking time (see e.g Ref. [7]).

[1] eV$_{\text{ee}}$ refers to the electron equivalent energy, and should be distinguished from the nuclear recoil energy, eV$_{\text{nr}}$ (see Sec. V).

IV. NEUTRINO OSCILLATIONS WITH A LIGHT STERILE NEUTRINO

In the present study, we employ a minimal extension of the standard model by considering a fourth light sterile neutrino state added to the three active neutrinos. In this case, neutrino flavor eigenstates ν_α, with $\alpha = \{e, \mu, \tau, s, \cdots\}$ are related to neutrino mass eigenstates ν_i, with $i = \{1, 2, 3, 4, \cdots\}$ through a unitary transformation as $\nu_\alpha = \sum_i U_{\alpha i} \nu_i$. Sterile neutrino mass schemes have been considered in the literature with various motivations. Attractive possibilities are the early 2+2 models [30, 31]. While they still constitute probably one of the most interesting sterile extensions of the standard model, their original motivation is gone. On the other hand, they are strongly restricted by solar and atmospheric data and do not allow for the eV-scale neutrino mass we are interested in here [32, 88, 89]. For this reason, we focus on the (3+1) scheme, which does allow for eV-neutrino masses as long as the doublet-singlet mixing angles are adequately small, so that the sterile state decouples from both solar and atmospheric conversions, a possibility absent in the 2+2 schemes.

The generated reactor antineutrinos $\bar{\nu}_e$ of energy E_ν are expected to travel the propagation distance L with the survival probability

$$P_{ee} = 1 - 4 \sum_{i=1}^{3} \sum_{j>i}^{4} \left|U_{ei}\right|^2 \left|U_{ej}\right|^2 \sin^2\left(\Delta_{ji}\right) , \tag{9}$$

where $\Delta_{ji} = \Delta m^2_{ji} L/4E_\nu$, with the mass splittings denoted as $\Delta m^2_{ji} = m_j^2 - m_i^2$. In this work we will consider values of Δm^2_{ji} of the order of 1 eV^2, as required in order to account for the current neutrino anomalies. The matrix elements entering Eq.(9) take the form

$$U_{e1} = \cos\theta_{14} \cos\theta_{13} \cos\theta_{12} , \tag{10}$$

$$U_{e2} = \cos\theta_{14} \cos\theta_{13} \sin\theta_{12} , \tag{11}$$

$$U_{e3} = \cos\theta_{14} \sin\theta_{13} , \tag{12}$$

$$U_{e4} = \sin\theta_{14} . \tag{13}$$

In this framework, the hypothesis of a fourth neutrino generation yields the approximate electron neutrino survival probability for a given value of (L/E_ν)

$$\begin{aligned}
P_{ee} \simeq 1 - & \cos^4\theta_{14} \sin^2 2\theta_{13} \sin^2\left(\frac{\Delta m^2_{31} L}{4E_\nu}\right) \\
& - \sin^2 2\theta_{14} \sin^2\left(\frac{\Delta m^2_{41} L}{4E_\nu}\right) .
\end{aligned} \tag{14}$$

Note that, for vanishing θ_{14} or neutrino paths larger than 100 m, the latter expression reduces to the well-known oscillation probability for short-baselines probed at the new generation of reactor experiments such as Daya Bay [46], RENO [47] and Double Chooz [48]. On the contrary, at shorter distances, atmospheric neutrino driven oscilla-

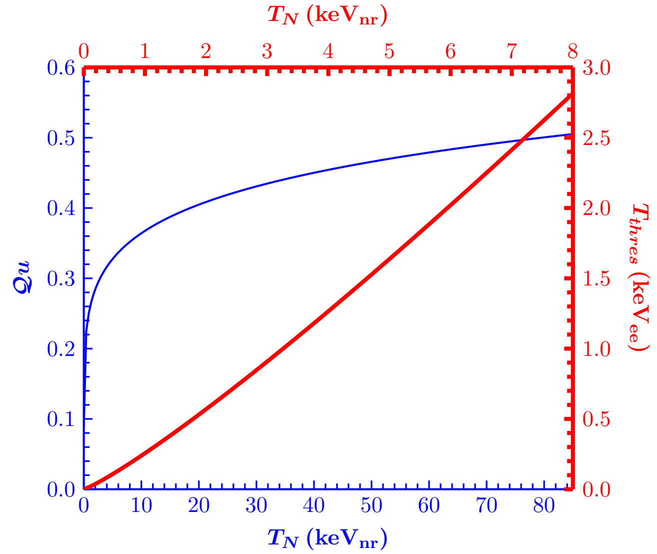

FIG. 1. (*Blue labeling*): The quenching factor, $\mathcal{Q}u(T_N)$ for ^{76}Ge and (*Red labeling*): the equivalent electron energy as a function of the nuclear recoil energy, T_N.

tions can be neglected and the neutrino survival probability can be effectively parametrized as

$$P_{ee} = 1 - \sin^2 2\theta_{14} \sin^2 \left(\frac{\Delta m_{41}^2 L}{4E_\nu} \right) . \tag{15}$$

V. NUMERICAL RESULTS

Reactor neutrino experiments are sensitive to the mixing matrix element U_{e4}, while SNS experiments are sensitive to both U_{e4} and $U_{\mu 4}$, through the measurement of $\sin^2 2\theta_{14}$. In the presence of sterile neutrinos, the differential event rate in terms of the nuclear recoil energy T_N, reads

$$\begin{aligned} \frac{dN^{events}_{\text{sterile}}}{dT_N} =& K \int_{E_{\nu_{\min}}}^{E_{\nu_{\max}}} dE_\nu \, \eta^{\lambda}_{\nu_\alpha}(E_\nu) P_{\alpha\alpha}(E_\nu) \\ & \times \int_{-1}^{1} d\cos\theta \, \frac{d\sigma_{\nu_\alpha}}{d\cos\theta} \delta \left(T_N - \frac{Q^2}{2M} \right) , \\ \lambda = & \text{react, SNS} , \end{aligned} \tag{16}$$

where M is the nuclear mass and $K = N_{targ} \Phi_{\nu_\alpha} t_{tot}$, with N_{targ} denoting the total number of atoms in the detector and t_{tot} the time window of exposure. The incident neutrino flux is given by Φ_{ν_α}, while $\eta^{\text{react}}_{\nu_\alpha}$ and $\eta^{\text{SNS}}_{\nu_\alpha}$ denote the neutrino energy-distributions at reactor experiments and SNS, respectively. Note that, in contrast to our previous studies [7, 70], the above expression includes the effect of flavor oscillations in the neutrino propagation. Then, the number of events for a given detector threshold, T_{thres}, is evaluated through the integral

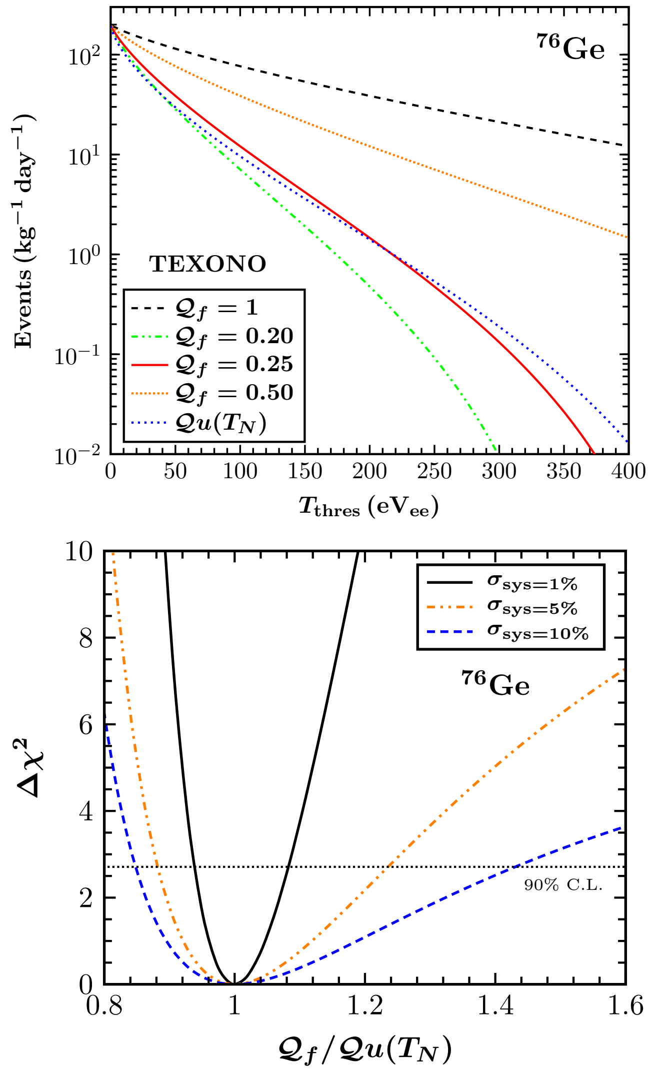

FIG. 2. Top panel: CEνNS events within the SM as a function of the detector threshold assuming different quenching factors and a 1kg-day ^{76}Ge target. A notable agreement is verified between the results obtained for the case of constant quenching factor in the range $\mathcal{Q}_f = 0.20 - 0.25$ and the empirical quenching factor of Eq.(18). Bottom panel: Sensitivity of the TEXONO experiment to the quenching factor $\mathcal{Q}_f$ normalized to the empirical quenching factor of Eq.(18) for various systematic errors and a background of 1 cpd (see the text).

$$N^{events}_{\text{sterile}} = \int_{T_{\text{thres}}}^{T_{\max}} \frac{dN^{events}_{\text{sterile}}}{dT_N} \, dT_N \, , \tag{17}$$

where $T_{\max}$ is the maximum recoil energy obtained from the kinematics of the process [5].

Focusing on the relevant CEνNS experiments, the detectable energy is lower than the energy imparted to the nuclear target (eV$_{\text{nr}}$), since the employed detectors are sensitive to an ionization energy equivalent to an electron energy (eV$_{\text{ee}}$) [90]. To account for the energy loss due to the conversion to phonons in such measurements, the

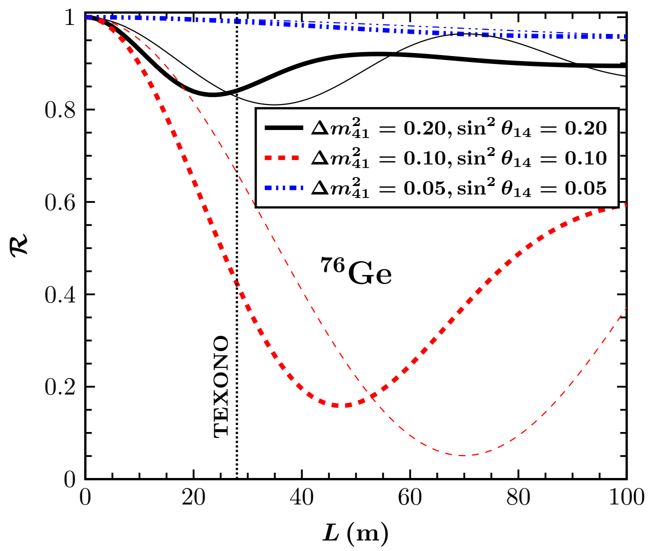

FIG. 3. Ratio $\mathcal{R} = N^{events}_{\rm sterile}/N^{events}_{\rm SM}$ for a detector threshold $T_{\rm thres} = 100$ eV$_{\rm ee}$ as a function of the baseline L, at the TEXONO experiment. The quenching effect is considered (neglected) in the thin (thick) lines. The vertical dotted line indicates the TEXONO baseline.

present calculations take into consideration the quenching effect on the nuclear recoil events by multiplying the energy scale by a quenching factor, $\mathcal{Q}_f$ [91]. In general, $\mathcal{Q}_f$ varies with the nuclear recoil energy and, usually, for its estimation the following empirical form is considered [92]:

$$\mathcal{Q}u(T_N) = r_1 \left[\frac{T_N}{1\text{keV}}\right]^{r_2}, \quad r_1 \simeq 0.256,\ r_2 \simeq 0.153\,. \tag{18}$$

The dependence of $\mathcal{Q}_f$ on the nuclear recoil energy, T_N, is shown in Fig. 1 where the equivalent electron energy as a function of T_N is also presented. The top panel of Fig. 2, illustrates the variation of the expected CEνNS event rates at different thresholds and quenching factors at the TEXONO reactor experiment. On the other hand, in the bottom panel of Fig. 2, based on the $\chi^2(\mathcal{Q}_f) = \min_\xi \left[\chi^2(\mathcal{Q},\xi)\right]$ function we examine how well the quenching factor is required to be known in order to record a clear signal, assuming SM interactions only. For this calculation, a 1 kg ^{76}Ge detector has been assumed with a threshold of 100 eV$_{\rm ee}$, one year of exposure and various systematic errors. Following Ref. [56], the considered background is set at 1 cpd e.g. 1 event day^{-1} kg^{-1} keV^{-1} ensuring a signal-to-noise ratio > 22 (for its spectral shape the reader is referred to Ref [71]).

In order to get an idea of how the presence of sterile neutrinos affects the expected number of events at a given detector, we define the ratio

$$\mathcal{R} = \frac{N^{events}_{\rm sterile}}{N^{events}_{\rm SM}}\,, \tag{19}$$

i.e., the portion of events originated from sterile neutrinos in the total number of SM events. We mention that $\mathcal{R}$ is independent of the detector mass and may also limit inevitable flux uncertainties. Apparently, the equality $\mathcal{R} = \langle\sigma\rangle_{\rm sterile} / \langle\sigma\rangle_{\rm SM}$ holds true, where $\langle\sigma\rangle_{\rm SM}$ stands for the SM cross section averaged over the reactor neutrino flux distribution, while $\langle\sigma\rangle_{\rm sterile}$ denotes the corresponding flux-averaged cross section that includes also the oscillation probability. Figure 3 shows the variation of $\mathcal{R}$ with the distance L for various choices of the sterile neutrino parameters, assuming a ^{76}Ge detector with mass 1 kg and an energy threshold of $T_{\rm thres} = 100$ eV$_{\rm ee}$ at the TEXONO experiment. The quenching effect is taken into account, while for comparison, the corresponding results obtained by neglecting the quenching effect are also illustrated.

The relevant experiments searching for CEνNS are subject to a number of uncertainties that should be effectively taken into account in order to come out with realistic estimates of the sensitivity to possible new physics phenomena. In such type of experiments the dominant contributions to systematic uncertainties are linked to the lack of precise knowledge on the neutrino flux, the quenching factor, the detector threshold, mass and performance, distance from the source, etc [71]. Background uncertainties depend on the various experimental setups and include mostly beam-related backgrounds (e.g. neutrino-induced neutrons), internal beta- and gamma-radioactivity and other secondary backgrounds from shielding materials [72]. Based on the pull method, in our attempt to quantify the sensitivity of a given CEνNS experiment to sterile neutrinos, we define the χ^2 function

$$\begin{aligned}\chi^2(\sin^2 2\theta, \Delta m^2_{41}) &= \min_\xi \left[\chi^2(\sin^2 2\theta, \Delta m^2_{41}, \xi)\right] \\ &= \min_\xi \left[\left(\frac{N^{events}_{\rm SM} - N^{events}_{\rm sterile}(1+\xi)}{\sigma_{\rm stat}}\right)^2 + \left(\frac{\xi}{\sigma_{\rm sys}}\right)^2\right],\end{aligned} \tag{20}$$

with $\sigma_{\rm stat} = \sqrt{N^{events}_{\rm SM} + N^{events}_{\rm bkg}}$, minimized over the nuisance parameter ξ. Following a conservative approach, in this work we adopt typical values to account for the systematic error, i.e. $\sigma_{\rm sys} = 10\%$. For the case of TEXONO we consider a background level of 1 cpd, while for the case of COHERENT we assume that the number of background events is of the order of 20% of the $N^{events}_{\rm SM}$ [59]. For convenience it is also useful to obtain the minimum χ^2 with respect to ξ analytically, as

$$\chi^2_{\rm min}(\sin^2 2\theta, \Delta m^2_{41}) = \frac{(N^{events}_{\rm SM} - N^{events}_{\rm sterile})^2}{\sigma^2_{\rm stat} + (\sigma_{\rm sys}\, N^{events}_{\rm sterile})^2}\,. \tag{21}$$

Note that, by neglecting the systematic uncertainty, the latter reduces to the simple χ^2 form employed in our previous works [7, 70].

We mention that, due to the smallness of θ_{13}, recently measured at Daya Bay [46], for simplicity in our calculations we set $\sin^2 2\theta_{13} = 0$. Moreover, we use the fact

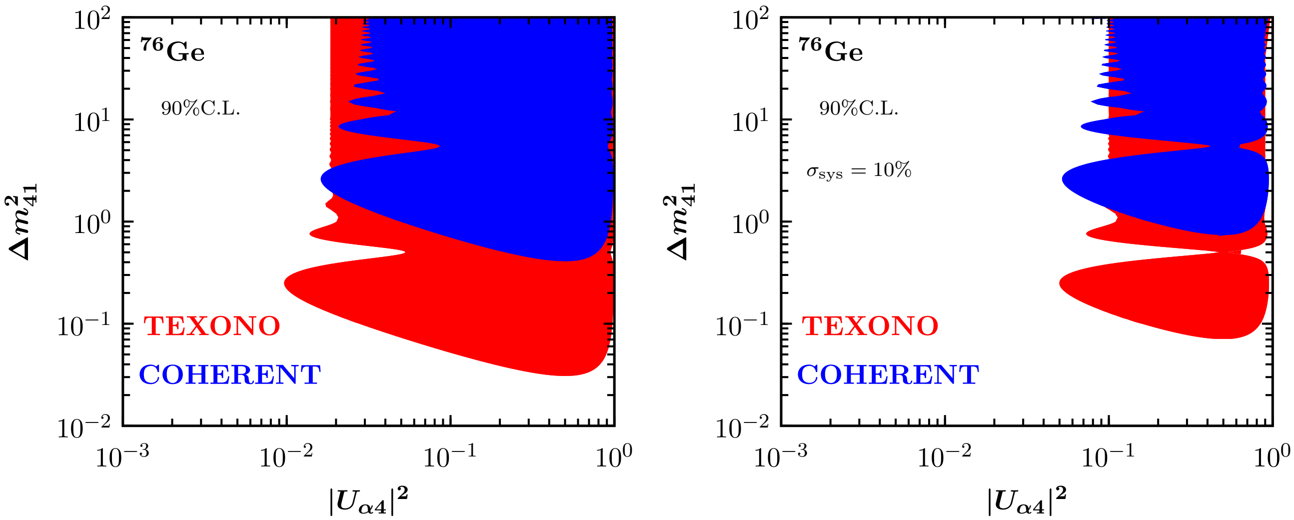

FIG. 4. 90% C.L. sensitivity regions in the ($|U_{\alpha 4}|^2$, Δm^2_{41}) planes with $\alpha = e$ (red region) and $\alpha = \mu$ (blue region) assuming a light sterile neutrino in the (3+1) scheme, at the TEXONO and COHERENT experiments respectively (for details see the text). In the left panel systematic uncertainties and background events are neglected, while in the right panel the calculation assumes a systematic error of $\sigma_{\rm sys} = 10\%$ for the corresponding background events in each experiment.

that, within the framework of the (3+1) scheme, it holds

$$\sin^2 2\theta_{\alpha\alpha} = 4|U_{\alpha 4}|^2 \left(1 - |U_{\alpha 4}|^2\right) , \tag{22}$$

$$\sin^2 2\theta_{\alpha\beta} = 4|U_{\alpha 4}|^2 |U_{\beta 4}|^2 , \tag{23}$$

where $\alpha, \beta = e, \mu, \tau, s$. Focusing on the relevant short-baseline (SBL) neutrino experiments, the above expressions enter into the respective effective survival and transition probabilities, valid for neutrinos and antineutrinos

$$\begin{aligned} P_{\alpha\alpha} &= 1 - \sin^2 2\theta_{\alpha\alpha} \sin^2\left(\frac{\Delta m^2_{41} L}{4E}\right) , \\ P_{\alpha\beta} &= \sin^2 2\theta_{\alpha\beta} \sin^2\left(\frac{\Delta m^2_{41} L}{4E}\right) . \end{aligned} \tag{24}$$

In Fig. 4 we illustrate the 90% C.L. sensitivity contours in the ($|U_{e4}|^2$, Δm^2_{41}) plane for the TEXONO experiment, obtained from a two-parameter χ^2 analysis as described above and by taking into account the quenching effect. The present calculations consider a ^{76}Ge detector with: 1 kg mass, 100 eV$_{\rm ee}$ energy threshold and one year of data collection time. For comparison, also shown is the corresponding sensitivity region in the ($|U_{\mu 4}|^2$, Δm^2_{41}) plane for the case of the COHERENT experiment assuming its "current" setup (see Sec. III).

Our present results indicate clearly that a dedicated experiment searching for CEνNS has also satisfactory capabilities to probe sterile neutrinos. For the case of the TEXONO experiment, the lack of $\bar{\nu}_e$ disappearance results in the sensitivity regions are depicted in the top panel of Fig. 5 after one year of data taking time by considering two extreme possibilities for the detector mass (e.g. 1 kg and 100 kg). In each case the assumed experimental setup consists of a ^{76}Ge detector with a 100 eV$_{\rm ee}$ threshold and a background level of 1 cpd. For comparison purposes, apart from the typical $\sigma_{\rm sys} = 10\%$, two additional more optimistic possibilities of the systematic error are also taken into account: $\sigma_{\rm sys} = 5\%$ and $\sigma_{\rm sys} = 1\%$. Moreover, we also explore a more conservative scenario by assuming a 10 cpd background level which shows differences only for the case of 1% systematic error. On the other hand, in the bottom panel of Fig. 5 by neglecting systematic errors and background events, the results are also illustrated for two different values of the ^{76}Ge target mass (1 kg and 100 kg) and four possible energy thresholds (1 eV$_{\rm ee}$, 10 eV$_{\rm ee}$, 100 eV$_{\rm ee}$, 400 eV$_{\rm ee}$). For these thresholds, by using Eq.(18) the corresponding quenching factors become $\mathcal{Q}u = (0.12, 0.16, 0.23, 0.27)$ leading to nuclear recoil thresholds (8 eV$_{\rm nr}$, 60 eV$_{\rm nr}$, 442 eV$_{\rm nr}$, 1472 eV$_{\rm nr}$), respectively. Note, that this is also consistent with the choice $\mathcal{Q}_f = 0.20 - 0.25$ employed in our previous work where we only considered a 100 eV$_{\rm ee}$ threshold [70]. We furthermore note that, by assuming a threshold as high as $T_{\rm thres} = 400$ eV$_{\rm ee}$, the results indicate that TEXONO has no sensitivity to sterile parameters for the case of 1 kg ^{76}Ge detector mass. One also sees that large values of $\sin^2 2\theta_{ee}$ would be ruled out by the exclusion curves, in agreement with the results of Refs. [25, 34]. In addition, as stated in Ref. [37], the requirement of large $|U_{e1}|^2 + |U_{e2}|^2$ for solar neutrino oscillations, implies that values of $|U_{e4}|^2$ close to unity are excluded. Therefore, for small $\sin^2 2\theta_{ee}$ one has

$$\sin^2 2\theta_{ee} \simeq 4|U_{e4}|^2 . \tag{25}$$

which satisfies the general expectation that the fourth generation massive neutrino is mostly sterile.

At this point we turn our attention on the capability of the COHERENT experiment [59] at the SNS, Oak

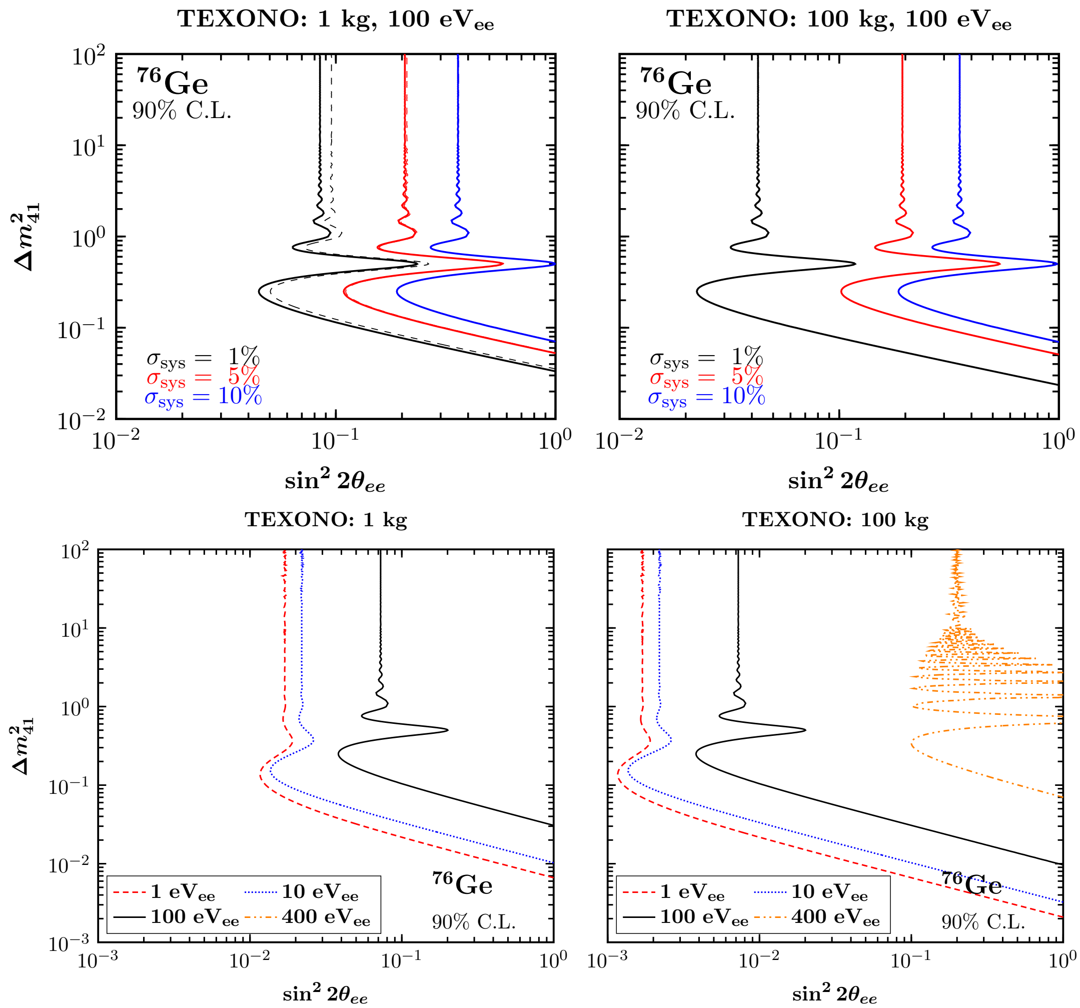

FIG. 5. Top panel: 90% C.L. sensitivity region in the $(\sin^2 2\theta_{ee}, \Delta m^2_{41})$ plane for a light sterile neutrino in the (3+1) scheme, considering the current experimental setup at the TEXONO experiment for different values of systematic error for a background level of 1 cpd (solid lines) and 10 cpd (dashed lines). Bottom panel: 90% C.L. sensitivity region for different configurations of detector mass and operation threshold with neglected background and systematic uncertainties.

Ridge, to probe the sterile neutrino parameters (for a comprehensive analysis, see also Ref. [8]). Although SNS experiments in general involve both U_{e4} and $U_{\mu 4}$, here we concentrate just on the latter since COHERENT is optimized to record muonic neutrino beams [70]. Focusing on various promising nuclear targets at the SNS, in Fig. 6 we illustrate the expected sensitivity of the COHERENT to sterile neutrino parameters in the $(\sin^2 2\theta_{\mu\mu}, \Delta m^2_{41})$ plane, by assuming only the $\bar{\nu}_\mu$ component of the delayed neutrino flux. For the sake of comparison, the bottom panel of Fig. 6 shows the corresponding sensitivity by neglecting systematic uncertainties and background events for the case of ^{76}Ge. The obtained results, in conjunction with the large values of $|U_{\mu 1}|^2 + |U_{\mu 2}|^2 + |U_{\mu 3}|^2$ that are indicated by atmospheric neutrino data [93], imply small values of $|U_{\mu 4}|^2$. Then, similarly to reactor neutrino experiments, one may write

$$\sin^2 2\theta_{\mu\mu} \simeq 4|U_{\mu 4}|^2 \,. \tag{26}$$

Furthermore, a combination of Eq.(23) with Eqs.(25) and (26) yields the appearance-disappearance constraint [94]

$$\sin^2 2\theta_{e\mu} = \frac{1}{4} \sin^2 2\theta_{ee} \sin^2 2\theta_{\mu\mu} \,, \tag{27}$$

which implies that $\sin^2 2\theta_{e\mu}$ is doubly suppressed for small values of $\sin^2 2\theta_{ee}$ and $\sin^2 2\theta_{\mu\mu}$. From the corresponding exclusion curve in Fig. 7 by assuming various nuclear targets and the previously described systematic uncertainties and backgrounds as well as in Fig. 8 for zero background events and statistical errors only, we find that a combined analysis leads to a high sensitivity for sterile neutrino searches. Confronting the present results with the respective allowed regions by LSND [21] and MiniBooNE [23, 24, 95] (see Figs. 7 and 8), we conclude that the expected sensitivity from CEνNS has the potential to probe them, especially after the future

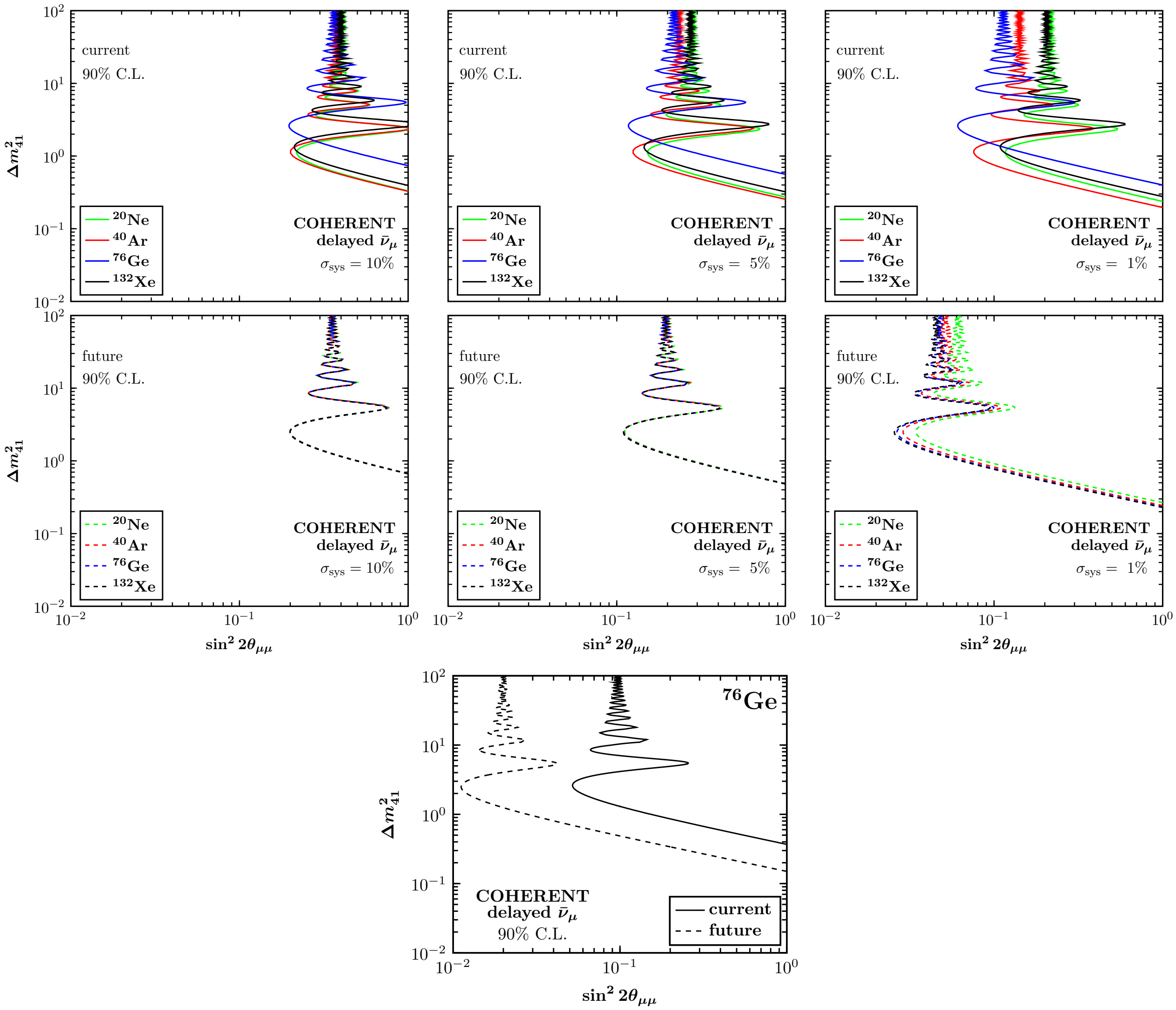

FIG. 6. Top panel: 90% C.L. sensitivity region in the $(\sin^2 2\theta_{\mu\mu}, \Delta m^2_{41})$ plane assuming a light sterile neutrino in the (3+1) scheme at the COHERENT experiment, for various nuclear targets. Different systematic uncertainties are considered while the assumed background events are 20% of the SM events. Only the delayed $\bar{\nu}_\mu$ beam is taken into account for the "current" and "future" experimental setup. Bottom panel: Same as above, but with zero systematic error and neglected backgrounds. The calculation refers to the case of a ^{76}Ge target only.

upgrade of COHERENT and TEXONO. These results are also competitive with recent sterile neutrino fits obtained from global analyses of SBL neutrino oscillation searches [34, 89].

VI. CONCLUSIONS

We have examined the potential of short-baseline coherent elastic neutrino-nucleus scattering experiments to probe effects associated to light sterile neutrinos. For definiteness we have focused on the normal (3+1) neutrino mass scheme. We have found that the planned TEXONO and COHERENT experiments offer good prospects of providing key information concerning the existence of light sterile neutrinos. From our present results we conclude that dedicated low-energy neutrino experiments looking for CEνNS events could be complementary to charged-current appearance and disappearance searches. We have also verified that, by employing high-purity Germanium detectors with sub-keV thresholds, better sensitivities can be reached on the sterile neutrino mixing parameters. Such measurements would provide a deeper understanding of neutrino interactions over a very wide energy range and could possibly provide evidence for new physics in the lepton sector.

ACKNOWLEDGEMENTS

Work supported by MINECO grants FPA2014-58183-P, Multidark CSD2009-00064, SEV-2014-0398, and the

PROMETEOII/2014/084 grant from Generalitat Valenciana. M. T. is also supported by the grant GV2016-142 (Generalitat Valenciana) and by a Ramón y Cajal contract (MINECO). One of us, DKP, wishes to thank Prof. O. Miranda for stimulating discussions and Dr. R. Fonseca for technical assistance. JWFV acknowledges Prof. W.C. Louis for providing relevant experimental data.

NOTE ADDED

Recently, the COHERENT collaboration announced the observation of CEνNS for the first time at a 6.7 sigma confidence level, using a low-background, 14.6 kg CsI[Na] scintillator [96]. This enhances the significance of our results related to the COHERENT experiment.

[1] K. Scholberg, Phys.Rev. **D73**, 033005 (2006), arXiv:hep-ex/0511042 [hep-ex].

[2] H. T. Wong, Nucl.Phys. **A844**, 229C (2010).

[3] S. Brice, R. Cooper, F. DeJongh, A. Empl, L. Garrison, *et al.*, Phys.Rev. **D89**, 072004 (2014), arXiv:1311.5958 [physics.ins-det].

[4] J. I. Collar, N. E. Fields, M. Hai, T. W. Hossbach, J. L. Orrell, C. T. Overman, G. Perumpilly, and B. Scholz, Nucl. Instrum. Meth. **A773**, 56 (2015), arXiv:1407.7524 [physics.ins-det].

[5] D. K. Papoulias and T. S. Kosmas, Phys. Lett. **B728**, 482 (2014), arXiv:1312.2460 [nucl-th].

[6] D. K. Papoulias and T. S. Kosmas, Phys. Lett. **B747**, 454 (2015), arXiv:1506.05406 [hep-ph].

[7] T. S. Kosmas, O. G. Miranda, D. K. Papoulias, M. Tortola, and J. W. F. Valle, Phys. Rev. **D92**, 013011 (2015), arXiv:1505.03202 [hep-ph].

[8] A. Anderson, J. Conrad, E. Figueroa-Feliciano, C. Ignarra, G. Karagiorgi, *et al.*, Phys.Rev. **D86**, 013004 (2012), arXiv:1201.3805 [hep-ph].

[9] B. Dutta, Y. Gao, R. Mahapatra, N. Mirabolfathi, L. E. Strigari, and J. W. Walker, Phys. Rev. **D94**, 093002 (2016), arXiv:1511.02834 [hep-ph].

[10] D. Z. Freedman, Phys.Rev. **D9**, 1389 (1974).

[11] D. L. Tubbs and D. N. Schramm, Astrophys. J. **201**, 467 (1975).

[12] A. Drukier and L. Stodolsky, Phys.Rev. **D30**, 2295 (1984).

[13] J. A. Formaggio, E. Figueroa-Feliciano, and A. J. Anderson, Phys. Rev. **D85**, 013009 (2012), arXiv:1107.3512 [hep-ph].

[14] T. Kajita, Rev. Mod. Phys. **88**, 030501 (2016).

[15] A. B. McDonald, Rev. Mod. Phys. **88**, 030502 (2016).

[16] D. Forero, M. Tortola, and J. Valle, Phys.Rev. **D90**, 093006 (2014), arXiv:1405.7540 [hep-ph].

[17] J. W. Valle and J. C. Romao, *Neutrinos in high energy and astroparticle physics*, 1st ed. (Wiley-VCH, Berlin, 2015).

[18] W. Hampel *et al.* (GALLEX), Phys. Lett. **B420**, 114 (1998).

[19] J. N. Abdurashitov *et al.* (SAGE Collaboration), Phys. Rev. **C80**, 015807 (2009), arXiv:0901.2200 [nucl-ex].

[20] C. Athanassopoulos *et al.* (LSND), Phys. Rev. Lett. **75**, 2650 (1995), nucl-ex/9504002.

[21] A. Aguilar *et al.* (LSND collaboration), Phys. Rev. **D64**, 112007 (2001), hep-ex/0104049.

[22] A. A. Aguilar-Arevalo *et al.* (MiniBooNE), Phys. Rev. Lett. **98**, 231801 (2007), arXiv:0704.1500 [hep-ex].

[23] A. A. Aguilar-Arevalo *et al.* (MiniBooNE) (2012) arXiv:1207.4809 [hep-ex].

[24] A. Aguilar-Arevalo *et al.* (MiniBooNE), Phys.Rev.Lett. **110**, 161801 (2013), arXiv:1207.4809 [hep-ex].

[25] G. Mention *et al.*, Phys. Rev. **D83**, 073006 (2011), arXiv:1101.2755 [hep-ex].

[26] T. Mueller, D. Lhuillier, M. Fallot, A. Letourneau, S. Cormon, *et al.*, Phys.Rev. **C83**, 054615 (2011), arXiv:1101.2663 [hep-ex].

[27] P. Huber, Phys. Rev. **C84**, 024617 (2011), [Erratum: Phys. Rev.C85,029901(2012)], arXiv:1106.0687 [hep-ph].

[28] M. Gonzalez-Garcia and M. Maltoni, Phys.Rept. **460**, 1 (2008), arXiv:0704.1800 [hep-ph].

[29] S. Gariazzo, C. Giunti, M. Laveder, Y. F. Li, and E. M. Zavanin, J. Phys. **G43**, 033001 (2016), arXiv:1507.08204 [hep-ph].

[30] J. T. Peltoniemi and J. W. F. Valle, Nucl. Phys. **B406**, 409 (1993), hep-ph/9302316.

[31] J. T. Peltoniemi, D. Tommasini, and J. W. F. Valle, Phys. Lett. **B298**, 383 (1993).

[32] M. Maltoni, T. Schwetz, M. Tortola, and J. W. F. Valle, New J.Phys. **6**, 122 (2004), this review gives a comprehensive set of references, arXiv:hep-ph/0405172 [hep-ph].

[33] A. de Gouvea and T. Wytock, Phys. Rev. **D79**, 073005 (2009), arXiv:0809.5076 [hep-ph].

[34] C. Giunti and M. Laveder, Phys. Rev. **D84**, 073008 (2011), arXiv:1107.1452 [hep-ph].

[35] J. Kopp, P. A. N. Machado, M. Maltoni, and T. Schwetz, JHEP **05**, 050 (2013), arXiv:1303.3011 [hep-ph].

[36] F. P. An *et al.* (Daya Bay), Phys. Rev. Lett. **113**, 141802 (2014), arXiv:1407.7259 [hep-ex].

[37] C. Giunti and E. M. Zavanin, Mod. Phys. Lett. **A31**, 1650003 (2016), arXiv:1508.03172 [hep-ph].

[38] J. Schechter and J. Valle, Phys.Rev. **D22**, 2227 (1980).

[39] R. N. Mohapatra and J. W. F. Valle, Phys. Rev. **D34**, 1642 (1986).

[40] E. Akhmedov *et al.*, Phys. Lett. **B368**, 270 (1996), hep-ph/9507275.

[41] E. Akhmedov *et al.*, Phys. Rev. **D53**, 2752 (1996), hep-ph/9509255.

[42] M. Malinsky, J. C. Romao, and J. W. F. Valle, Phys. Rev. Lett. **95**, 161801 (2005).
[43] J. Lesgourgues, G. Mangano, G. Miele, and S. Pastor, *Neutrino Cosmology* (Cambridge University Press, Cambridge, England, 2013).
[44] C. Giunti, Nucl. Phys. **B908**, 336 (2016), arXiv:1512.04758 [hep-ph].
[45] P. C. de Holanda and A. Yu. Smirnov, Phys. Rev. **D83**, 113011 (2011), arXiv:1012.5627 [hep-ph].
[46] F. P. An *et al.* (Daya Bay), Phys. Rev. Lett. **112**, 061801 (2014), arXiv:1310.6732 [hep-ex].
[47] J. Ahn *et al.* (RENO collaboration), Phys.Rev.Lett. **108**, 191802 (2012), arXiv:1204.0626 [hep-ex].
[48] Y. Abe *et al.* (DOUBLE-CHOOZ Collaboration), Phys.Rev.Lett. **108**, 131801 (2012), arXiv:1112.6353 [hep-ex].
[49] A. Bandyopadhyay *et al.* (ISS Physics Working Group), Rept.Prog.Phys. **72**, 106201 (2009), arXiv:0710.4947 [hep-ph].
[50] A. B. Balantekin and N. Vassh, Phys. Rev. **D89**, 073013 (2014), arXiv:1312.6858 [hep-ph].
[51] S. Ando and A. Kusenko, Phys. Rev. **D81**, 113006 (2010), arXiv:1001.5273 [hep-ph].
[52] W. Liao, X.-H. Wu, and H. Zhou, Phys. Rev. **D89**, 093017 (2014), arXiv:1311.6075 [hep-ph].
[53] S. M. Bilenky, C. Giunti, J. A. Grifols, and E. Masso, Phys. Rept. **379**, 69 (2003), hep-ph/0211462.
[54] J. D. Vergados, H. Ejiri, and F. Simkovic, Rept. Prog. Phys. **75**, 106301 (2012), arXiv:1205.0649 [hep-ph].
[55] C. Giunti and M. Laveder, Phys. Rev. **D82**, 053005 (2010), arXiv:1005.4599 [hep-ph].
[56] A. K. Soma *et al.* (TEXONO), Nucl. Instrum. Meth. **A836**, 67 (2016), arXiv:1411.4802 [physics.ins-det].
[57] B. Dutta, R. Mahapatra, L. E. Strigari, and J. W. Walker, Phys. Rev. **D93**, 013015 (2016), arXiv:1508.07981 [hep-ph].
[58] J.-W. Chen, H.-C. Chi, S.-T. Lin, C. P. Liu, L. Singh, H. T. Wong, C.-L. Wu, and C.-P. Wu, Phys. Rev. **D93**, 093012 (2016), arXiv:1601.07257 [hep-ph].
[59] D. Akimov *et al.* (COHERENT), (2015), arXiv:1509.08702 [physics.ins-det].
[60] S. Kerman, V. Sharma, M. Deniz, H. T. Wong, J. W. Chen, H. B. Li, S. T. Lin, C. P. Liu, and Q. Yue (TEXONO), Phys. Rev. **D93**, 113006 (2016), arXiv:1603.08786 [hep-ph].
[61] B. Sevda, M. Deniz, S. Kerman, L. Singh, H. T. Wong, and M. Zeyrek, Phys. Rev. **D95**, 033008 (2017), arXiv:1611.07259 [hep-ex].
[62] V. Belov *et al.*, JINST **10**, P12011 (2015).
[63] A. G. Beda, V. B. Brudanin, V. G. Egorov, D. V. Medvedev, V. S. Pogosov, E. A. Shevchik, M. V. Shirchenko, A. S. Starostin, and I. V. Zhitnikov, Phys. Part. Nucl. Lett. **10**, 139 (2013).
[64] G. Fernandez Moroni, J. Estrada, E. E. Paolini, G. Cancelo, J. Tiffenberg, and J. Molina, Phys. Rev. **D91**, 072001 (2015), arXiv:1405.5761 [physics.ins-det].
[65] A. Aguilar-Arevalo *et al.* (CONNIE), JINST **11**, P07024 (2016), arXiv:1604.01343 [physics.ins-det].
[66] G. Agnolet *et al.* (MINER), Nucl. Instrum. Meth. **A853**, 53 (2017), arXiv:1609.02066 [physics.ins-det].
[67] J. Billard *et al.*, J. Phys. **G44**, 105101 (2017), arXiv:1612.09035 [physics.ins-det].
[68] R. Strauss *et al.*, Eur. Phys. J. **C77**, 506 (2017), arXiv:1704.04320 [physics.ins-det].
[69] D. K. Papoulias and T. S. Kosmas, Adv. High Energy Phys. **2015**, 763648 (2015), arXiv:1502.02928 [nucl-th].
[70] T. S. Kosmas, O. G. Miranda, D. K. Papoulias, M. Tortola, and J. W. F. Valle, Phys. Lett. **B750**, 459 (2015), arXiv:1506.08377 [hep-ph].
[71] M. Lindner, W. Rodejohann, and X.-J. Xu, JHEP **03**, 097 (2017), arXiv:1612.04150 [hep-ph].
[72] J. B. Dent, B. Dutta, S. Liao, J. L. Newstead, L. E. Strigari, and J. W. Walker, (2016), arXiv:1612.06350 [hep-ph].
[73] P. Coloma, P. B. Denton, M. C. Gonzalez-Garcia, M. Maltoni, and T. Schwetz, JHEP **04**, 116 (2017), arXiv:1701.04828 [hep-ph].
[74] P. Giannaka and T. Kosmas, Advances in High Energy Physics **2015**, 398796 (2015), arXiv:1502.07225 [nucl-th].
[75] V. Chasioti and T. Kosmas, Nucl.Phys. **A829**, 234 (2009).
[76] J. Beringer *et al.* (Particle Data Group), Phys.Rev. **D86**, 010001 (2012).
[77] R. Machleidt, K. Holinde, and C. Elster, Phys. Rept. **149**, 1 (1987).
[78] V. G. J. Stoks, R. A. M. Klomp, C. P. F. Terheggen, and J. J. de Swart, Phys. Rev. **C49**, 2950 (1994), arXiv:nucl-th/9406039 [nucl-th].
[79] R. Machleidt, Phys. Rev. **C63**, 024001 (2001), arXiv:nucl-th/0006014 [nucl-th].
[80] T. S. Kosmas and J. D. Vergados, Nucl. Phys. **A536**, 72 (1992).
[81] T. S. Kosmas, S. Kovalenko, and I. Schmidt, Phys. Lett. **B519**, 78 (2001), arXiv:hep-ph/0107292 [hep-ph].
[82] T. S. Kosmas and J. D. Vergados, Phys. Lett. **B217**, 19 (1989).
[83] V. Tsakstara and T. S. Kosmas, Phys. Rev. **C83**, 054612 (2011).
[84] V. I. Kopeikin, L. A. Mikaelyan, and V. V. Sinev, Phys. Atom. Nucl. **60**, 172 (1997).
[85] Y. Efremenko and W. Hix, J.Phys.Conf.Ser. **173**, 012006 (2009), arXiv:0807.2801 [nucl-ex].
[86] A. Aguilar-Arevalo *et al.* (MiniBooNE), Phys.Rev. **D79**, 072002 (2009), arXiv:0806.1449 [hep-ex].
[87] W. Louis, Prog.Part.Nucl.Phys. **63**, 51 (2009).
[88] M. Maltoni, T. Schwetz, M. A. Tortola, and J. W. F. Valle, (2003), hep-ph/0305312.
[89] J. Kopp, M. Maltoni, and T. Schwetz, Phys. Rev. Lett. **107**, 091801 (2011), arXiv:1103.4570 [hep-ph].
[90] Y. Giomataris and J. D. Vergados, Phys. Lett. **B634**, 23 (2006), arXiv:hep-ex/0503029 [hep-ex].
[91] J. D. Vergados, F. T. Avignone, III, and I. Giomataris, Phys. Rev. **D79**, 113001 (2009), arXiv:0902.1055 [hep-ph].
[92] E. Simon *et al.*, Nucl. Instrum. Meth. **A507**, 643 (2003), arXiv:astro-ph/0212491 [astro-ph].
[93] M. Maltoni and T. Schwetz, Phys. Rev. **D76**, 093005 (2007), arXiv:0705.0107 [hep-ph].
[94] S. M. Bilenky, C. Giunti, and W. Grimus, Eur. Phys. J. **C1**, 247 (1998), arXiv:hep-ph/9607372 [hep-ph].
[95] A. A. Aguilar-Arevalo *et al.* (MiniBooNE), Phys. Rev. Lett. **105**, 181801 (2010), arXiv:1007.1150 [hep-ex].
[96] D. Akimov *et al.* (COHERENT), Science (2017), 10.1126/science.aao0990, arXiv:1708.01294 [nucl-ex].

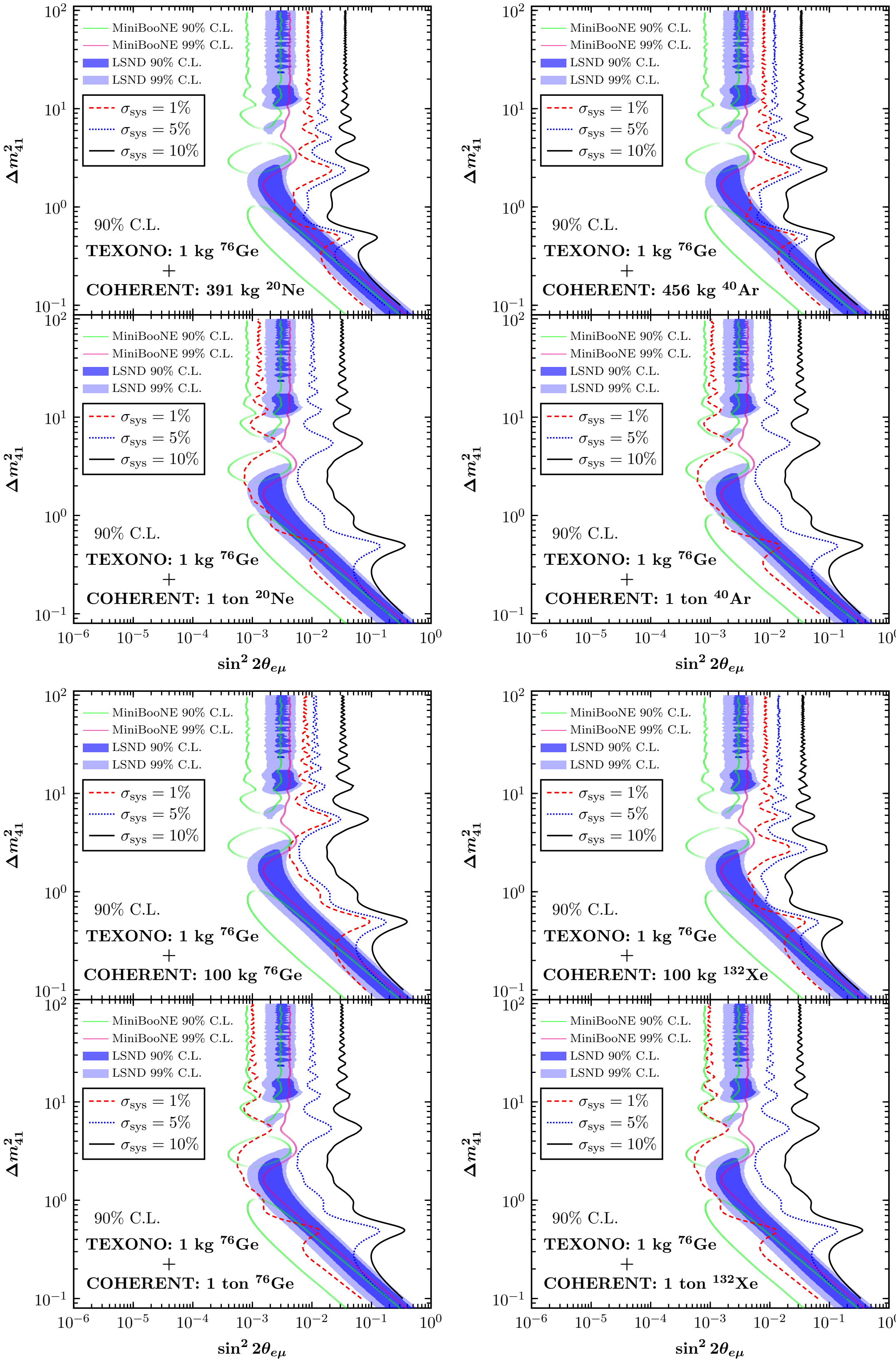

FIG. 7. 90% C.L sensitivity regions in the ($\sin^2 2\theta_{e\mu}$, Δm^2_{41}) plane from a combined analysis of COHERENT and TEXONO in the (3+1) scheme. Different experimental setups for the COHERENT experiment have been considered incorporating systematic uncertainties and backgrounds. For comparison the latest allowed regions from the LSND [20, 21] and MiniBooNE [23, 24] experiments are also shown.

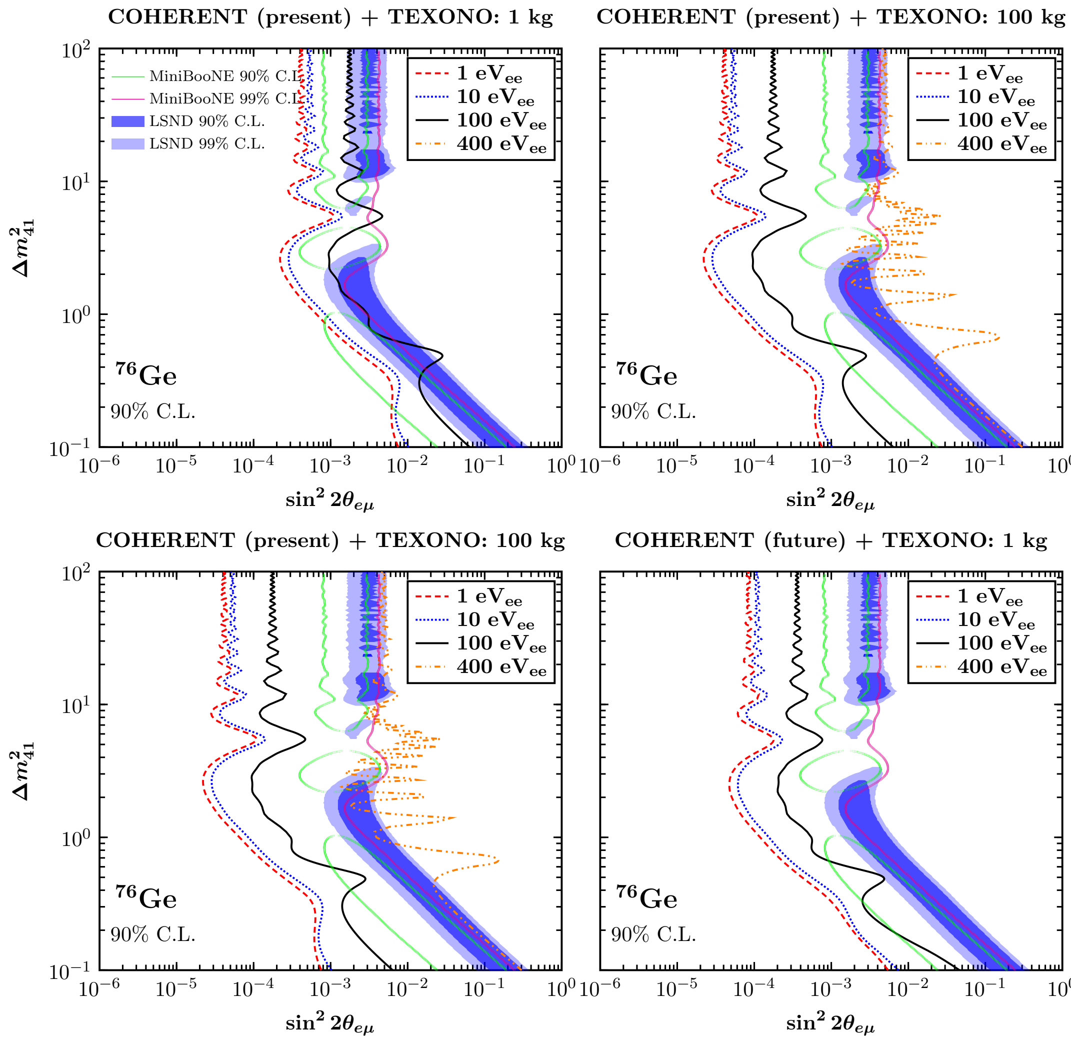

FIG. 8. Same as Fig. 7, considering different setups for TEXONO and COHERENT and neglecting systematic uncertainties and backgrounds. For COHERENT, we are assuming ^{76}Ge as target material.